Proc. Natl. Acad. Sci. USA
Vol. 93, pp. 6775–6779, June 1996
Biophysics

The kinesin walk: A dynamic model with elastically coupled heads

IMRE DERÉNYI AND TAMÁS VICSEK

Department of Atomic Physics, Eötvös University, Budapest, Puskin u 5–7, 1088 Hungary

Communicated by Leo P. Kadanoff, University of Chicago, Chicago, IL, February 26, 1996 (received for review November 28, 1995)

ABSTRACT **Recently individual two-headed kinesin molecules have been studied in *in vitro* motility assays revealing a number of their peculiar transport properties. In this paper we propose a simple and robust model for the kinesin stepping process with elastically coupled Brownian heads that show all of these properties. The analytic and numerical treatment of our model results in a very good fit to the experimental data and practically has no free parameters. Changing the values of the parameters in the restricted range allowed by the related experimental estimates has almost no effect on the shape of the curves and results mainly in a variation of the zero load velocity that can be directly fitted to the measured data. In addition, the model is consistent with the measured pathway of the kinesin ATPase.**

Kinesin is a motor protein that converts the energy of ATP hydrolysis into mechanical work while moving large distances along microtubule filaments and transporting organelles and vesicles inside the cytoplasm of eukaryotic cells (1). The wall of a microtubule is made up of tubulin heterodimers arranged in 13 longitudinal rows called protofilaments (Fig. 1). A tubulin heterodimer is 8 nm long and consists of two globular proteins about 4 nm in diameter: α- and β-tubulin. The dimers bind head-to-tail, giving the polarity to the protofilaments. The microtubule has a helical surface lattice that can have two possible configurations: the adjacent protofilaments can be shifted in the longitudinal direction by about either 5 nm (A-type lattice) or 1 nm (B-type lattice). Electron micrograph measurements of microtubules decorated with kinesin head fragments (2–5) indicate the predominance of the B-type lattice and show that kinesin heads can bind only to the β-tubulin (meanwhile weakly interacting with the α-tubulin also). Native kinesin is a dimeric molecule with two globular ($\approx 9 \times 3 \times 3$ nm) heads. Each one has an ATP and a tubulin binding site.

Recent experimental studies in *in vitro* motility assays have revealed the following properties of kinesin movement: (*i*) kinesin moves unidirectionally parallel to the protofilaments toward the "(+)" end of the microtubule (6, 7); (*ii*) under an increasing load the speed of the kinesin decreases almost linearly (8, 9) (see Fig. 3); (*iii*) under its stall force (about 5 pN) kinesin still consumes ATP at an elevated rate (9); (*iv*) in the absence of ATP (in rigor state) kinesin binds to the microtubule very strongly–it supports forces in excess of 10 pN (9); (*v*) the observed step size in the low speed regime (at low ATP or at high force) is about 8 nm (10); (*vi*) some backward slippage was clearly observed (9); and (*vii*) the displacement variance at saturating ATP and at low load increases linearly with time, but at (only somewhat more than) half of the rate of a single Poisson stepping process with 8 nm step size, implying that one step consists of two sequential subprocesses with comparable limiting rates (11).

Partially motivated by these remarkable experimental advances, several interesting thermal ratchet type models have very recently been developed for the theoretical interpretation of the related transport phenomena. These models (12–19), except that of Ajdari (20), consider cases in which the internal degree of freedom of the molecular motors is not taken into account. The purpose of the present work is to define and investigate a dynamic model for the kinesin walk that has an internal degree of freedom and results in a full agreement with the experimental data for the range of its parameters allowed by the known estimates for the lower and upper bounds of these parameters.

There are two basic classes of possible models for the stepping of kinesin (21). The first one is the "long-stride" model in which the heads are moving along a single protofilament. The two heads are displaced from each other by 8 nm. During the stepping process the back head passes the bound front head, advancing 16 nm. Then the heads change their roles and a new step may take place. However, within this framework, during the long stride the back head has a good chance to bind to a β site belonging to a neighboring track that is closer than the next β site in the same track. Another problem is that the low displacement variance observed experimentally cannot be naturally explained. This model was studied in detail by Peskin and Oster (22) who, by introducing several reaction rate constants, found a reasonable agreement with the experimental results.

The other possibility is the family of "two-step" models. These models naturally explain the low displacement variance due to the two sequential subprocesses. During one cycle one of the two heads takes a 8-nm step first then the other head steps. Note that the motion of just one head advances the centroid of the molecule by only 4 nm, the successive steps of the two heads in rapid pair results in an effective 8-nm step that can be observed in the low-speed regime. This kind of motion gives large stability to the protofilament tracking. The differences in the two-step models arise from the relative positions of the heads. If both heads track the same protofilament they are not able to pass each other, so we can always distinguish the front and the back head. In this case the distance of the heads alternates between 8 and 16 nm, which seems a bit large for the kinesin molecule with its 9- to 10-nm-long heads, but is still possible. (Alternating between 0 and 8 nm is already impossible because only one head can bind to each β-tubulin site at a time.) Another quite reasonable situation is when the *two heads track adjacent protofilaments* on a B-type lattice. In this case the heads are sitting on adjacent β-tubulins displaced from each other by only about 1 nm in the longitudinal direction; thus either can take the first step (they can be identical).

Dynamics of the Kinesin Walk

We present here a one-dimensional kinesin walk model that describes the whole family of two-step models. Each of the two Brownian heads can move along its own one-dimensional periodic potential with period $L = 8$ nm in an overdamped environment. The two potentials can be shifted relatively to each other by an arbitrary distance (or even can be the same). These potentials represent the interaction with the protofilaments, and the periods are the tubulin heterodimers. Each period has a deep potential valley corresponding to the binding site of the β-tubulin, and the other parts of the potential are flat. Each valley has an asymmetric "V" shape (see Fig. 2): the

The publication costs of this article were defrayed in part by page charge payment. This article must therefore be hereby marked "*advertisement*" in accordance with 18 U.S.C. §1734 solely to indicate this fact.

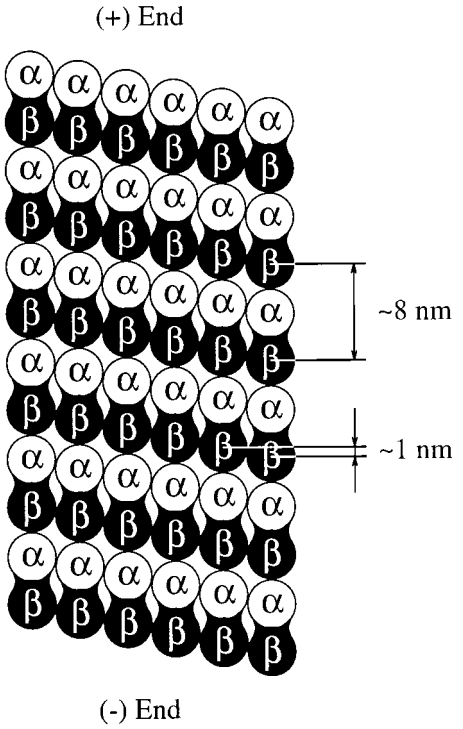

FIG. 1. Structure of the B-type helical surface lattice of the microtubule. The kinesin heads can bind only to the β-tubulin monomers.

slope in the backward direction [toward the "(−)" end of the microtubule] is steeper and 0.5–1 nm long, while the other slope [toward the "(+)" end] is 1.5–2 nm long, which shows the polarity of the filaments. These ranges are in the order of the Debye length.

In our model the heads are connected at a hinge, and a *spring acts between them* (Fig. 2). At the beginning of the mechanochemical cycle both heads are sitting in their valleys waiting for an ATP molecule, and the spring is unstrained. Any configuration of the model is mathematically equivalent to a model in which the two potentials are identical, the heads are sitting in the same valley, and therefore the rest length of the spring is zero. (Later we will consider only this version of the model.) After one of the heads binds an ATP molecule, the hydrolysis of this ATP causes a conformational change in this head—more precisely, it induces the head to take a 8-nm forward step. In the language of the model it means that the rest length of the spring changes from zero to 8 nm right after the hydrolysis. Then, as the first rate-limiting subprocess, the strained spring is trying to stretch, thus pushing the head to the next valley. Reaching its new 8-nm rest length another conformational change occurs in the head as a consequence of the ADP release: the rest length of the spring changes back to zero quickly; then, as the second rate-limiting subprocess, the spring is trying to contract pulling forward the other head. Completing the contraction a next cycle can start waiting for a new ATP molecule. Hirose *et al.* (5) provide evidence that the kinesin·ADP complex has indeed a different conformation near the junction of the heads. [Similarly, a myosin head also gets over several conformational changes (23, 24).] An important cooperative feature of our model is that only one ATP hydrolysis can occur during each cycle.

This picture is consistent with the scheme of Gilbert *et al.* (25) for the pathway of the kinesin ATPase. The first rate-limiting subprocess was observed as the dissociation of the head from the microtubule followed by a fast rebinding. They did not report on the second one, but it is clear that this subprocess already does not belong to the chemical part of the cycle and induces a slow dissociation and a fast rebinding of the other head.

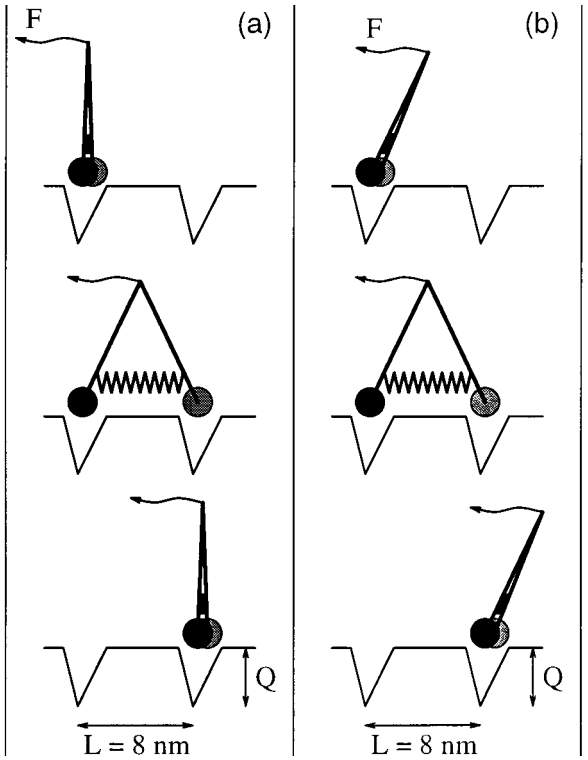

FIG. 2. Schematic picture of the potential and the subsequent steps (from top to bottom) of the kinesin molecule in the two limiting cases. In case *a* the hinge is always in the centroid of the molecule, and advances 4 nm during both subprocesses. The two heads share the load force equally. In case *b* the relative position of the hinge to the back head is fixed, thus the whole load force acts on this head. During the first subprocess the hinge does not move; however, during the second it advances 8 nm. All the intermediate cases are possible between *a* and *b*.

We can take the load force into account in a natural way. Since in the experiments of Svoboda *et al.* (9, 10) a large ($\approx$0.5 μm in diameter) and therefore slow (compared to the kinesin heads) silica bead was linked to the hinge of the kinesin molecule by a relatively weak elastic tether, we can apply a constant (independent of time) force F to the hinge. We arrive at the same conclusion by considering the experiments of Hunt *et al.* (8), where a viscous load acted on the moving microtubule while the long tail of the kinesin was fixed. But how can we transfer the force to the heads when writing down the equations of their motion? There are two possible limiting cases: if the hinge is always in the centroid of the molecule (Fig. 2*a*) the two heads share the load force equally (i.e., $F/2$ force acts on both heads); if the head that wants to step is always free from the load force (as in Fig. 2*b*), the whole force F acts on the actual back head. Due to the robustness of the model both (and therefore all the intermediate) cases yield practically the same force-velocity curves (Fig. 3).

The motion of the heads are described by the Langevin equations:

$$\begin{aligned}\Gamma\dot{x}_1 &= -\partial_x V(x_1) - F_1^{\text{load}} + K\cdot[x_2 - x_1 - l(t)] + \xi_1(t),\\ \Gamma\dot{x}_2 &= -\partial_x V(x_2) - F_1^{\text{load}} + K\cdot[x_1 - x_2 - l(t)] + \xi_2(t),\end{aligned} \quad [1]$$

where x_1 and x_2 denote the positions of the heads, Γ is the frictional drag coefficient, $V(x)$ is the periodic potential, $l(t)$ is the rest length (which alternates between 0 and 8 nm due to the conformational changes) and K is the stiffness of the spring, and $\xi_1(t)$, $\xi_2(t)$ are Gaussian white noises with the autocorrelation function $\langle\xi_j(t)\xi_i(t')\rangle = 2kT\Gamma\delta_{j,i}\delta(t - t')$ for $i, j = 1,2$.

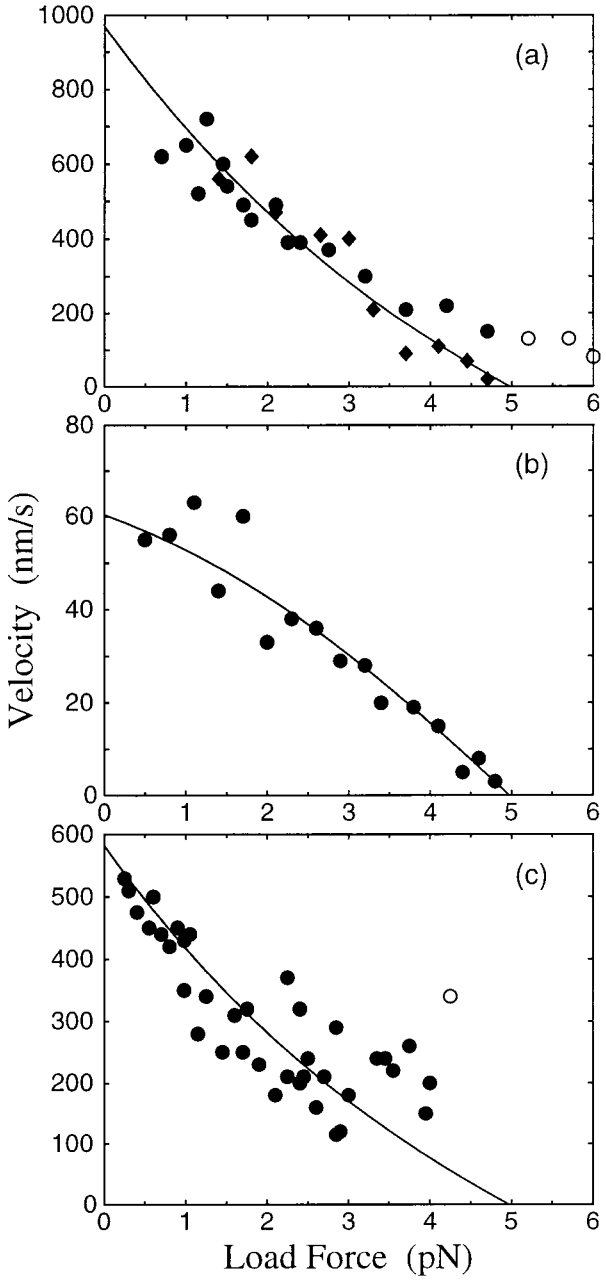

FIG. 3. The force-velocity curves for an individual kinesin molecule at saturating ($\gg$90 μM) ATP in *a* and *c*; and at low ($\approx$10 μM) ATP concentration in *b*. The experimental data (scattered symbols) are from Svoboda and Block (9) in *a* and *b* obtained by using optical tweezers; and from Hunt *et al.* (8) in *c*, applying viscous load. Open circles correspond to the simultaneous effect of multiple kinesin motors in the authors' interpretation (8, 9). Circles and diamonds in *a* mean two different set of the measured data. To get the best fit (solid lines), we chose 0.7 nm for the backward length of the potential valleys and 1.75 nm for the forward length; the depth of the valleys was $Q = 20kT$. In these plots the load force was $F/2$ on each kinesin head. In plot *b* we multiplied the average displacement by the ATP consumption rate $\nu(c_{\mathrm{ATP}}) = 10$ 1/s for the best fit. In plot *c* we used the same curve as in *a* but multiplied by a factor 0.6, which can be explained with the larger viscosity.

Results

To obtain results we can compare with the experiments first the values of the input parameters have to be specified. The drag coefficient Γ for a single head can be calculated from the Stokes formula yielding $\Gamma \approx 6 \times 10^{-11}$ kg/s.

The free energy that can be gained from the ATP hydrolysis is about $25kT$ or 100×10^{-21} J. During a stepping cycle the two conformational changes consume the free energy of the ATP, while the rest length of the spring changes by 8 nm in both cases. This means that $[1/2]\cdot 25kT \approx (K/2)(8\ \mathrm{nm})^2$, from which we get $K \approx 1.5$ pN/nm.

A lower limit for the depth Q of the potential valleys can be determined from the fact that the kinesin in rigor state supports forces in excess of 10 pN. If we try to pull out the two-headed kinesin molecule (with drag coefficient 2Γ) from a $2Q$ deep potential valley with a force F, a low limit for the escape rate is

$$\frac{F^2}{kT2\Gamma}e^{-2Q/kT}$$

as follows from a more general expression (Eq. **2**) to be discussed later. Assuming that the escape rate is much larger than 10^{-2} 1/s we get $13kT$ as a lower limit of Q. In reality the two heads cannot be handled as one larger head because they are not fixed to each other too rigidly; therefore, this is a very low limit. $Q \approx 20kT$ is expected to be a better estimate.

Note that the temperature T plays an important role in our model due to the deep potential valley the Brownian kinesin heads have to escape from.

We can assume that at the beginning of a stepping cycle both heads are sitting in the same valley of the potential. After the ATP hydrolysis, as the first conformational change, the strained spring is trying to stretch, pushing one of the heads to a neighboring valley, which is $L = 8$ nm away. If the load force is small there is a large probability $p^+_{0L} = J^+_{0L}/(J^+_{0L} + J^-_{0L})$ that the front head jumps to the forward direction due to the asymmetry of the potential valleys (the forward slope is less steep than the backward), and there is only a small probability $p^-_{0L} = J^-_{0L}/(J^+_{0L} + J^-_{0L})$ that the other head jumps backward. J^+_{0L} and J^-_{0L} denote the corresponding jumping rates. Increasing the load, the probability of the forward step decreases while that of the backward step increases. The average time $t_{0L} = 1/(J^+_{0L} + J^-_{0L})$ that is needed for this stretching also slightly increases. Completing this subprocess, the second conformational change occurs: the spring is trying to contract. Now for low load force the probability $p^+_{L0} = J^+_{L0}/(J^+_{L0} + J^-_{L0})$ that the backward head jumps forward to the next valley, where the other head is sitting, is close to 1, while the probability $p^-_{L0} = J^+_{L0}/(J^+_{L0} + J^-_{L0})$ that the forward head jumps backward is very small. Increasing the load the situation is similar to the previous case.

Thus, under low load force the kinesin molecule steps 8 nm forward during almost each mechanochemical cycle. But increasing the load the probability that the molecule remains on the same place or even takes a backward 8 nm step increases. Reaching the stall load the average displacement of the kinesin becomes zero.

Because the potential valleys are very deep (compared to the thermal energy kT), the heads spend almost all of their time at the bottom, and they are able to jump only very seldom. Therefore, we can calculate the above mentioned jumping rates ($J = J^+_{0L}, J^-_{0L}, J^+_{L0}$, or J^-_{L0}) from an Arrhenius-like formula. All we need for this is the effective potential $V^{\mathrm{eff}}(x)$ for the jumping head at the bottom of the valley and at the top of the barrier. The effective potential consists of five parts: the $V(x)$ periodic potential for the jumping head; the potential $F^{\mathrm{load}}_j x$ of the external load force; the spring potential $\langle (K/2)[x - x_r - l(t)]^2\rangle_{x_r}$; the $\langle V(x_r)\rangle_{x_r}$ potential for the remaining head; and the potential $\langle F^{\mathrm{load}}_r x_r\rangle_{x_r}$ of the external load force for the remaining head. In this approximation $\langle \dots \rangle_{x_r}$ means thermal averaging for the position x_r of the remaining head at the bottom of its valley. Thus, from the corresponding Fokker–Planck equation the jumping rate is

$$J = \frac{D \cdot e^{-(V_{\max}^{\text{eff}} - V_{\min}^{\text{eff}})/kT}}{\int e^{-[V^{\text{eff}}(x) - V_{\min}^{\text{eff}}]/kT} dx \cdot \int e^{-[V_{\max}^{\text{eff}} - V^{\text{eff}}(x)]/kT}\, dx}, \qquad [2]$$

where $D = kT/\Gamma$ denotes the diffusion coefficient; $V_{\min}^{\text{eff}}$ and $V_{\max}^{\text{eff}}$ are the minimal and the maximal values of the effective potential; and the integrals should be evaluated around the appropriate extremum. Due to the depth of the potential valleys, if we do not average the position of the remaining head but assume that it always sits at the bottom, we get similar results.

From the jumping rates one can calculate the average displacement $d = (p_{0L}^{+}p_{L0}^{+} - p_{0L}^{-}p_{L0}^{-})L = (J_{0L}^{+}J_{L0}^{+} - J_{0L}^{-}J_{L0}^{-})[1/(J_{0L}^{+} + J_{0L}^{-})][1/(J_{L0}^{+} + J_{L0}^{-})]L$ during a cycle and the average time $t = t_{0L} + t_{L0} = 1/(J_{0L}^{+} + J_{0L}^{-}) + 1/(J_{L0}^{+} + J_{L0}^{-})$ needed for this. Increasing the load, the average displacement decreases due to the increasing probabilities of the remaining and the backward slippage, and the average time slightly increases as a manifestation of the so-called Fenn effect (26). (At stall load it is about three times larger than without load.)

At saturating ATP concentration the only rate-limiting factor is the stepping process, therefore dividing the average displacement by the average time gives the average velocity $v = d/t$ of the kinesin (Fig. 3 *a* and *c*).

But at low ATP concentration the rate-limiting factor is the diffusion of the ATP to the kinesin heads—i.e., the stepping process is much faster than getting an ATP. Thus the average velocity is proportional to the average displacement during one cycle with the prefactor

$$\nu(c_{\text{ATP}}) = \frac{\nu_{\text{sat}} \cdot c_{\text{ATP}}}{K_{\text{m}} + c_{\text{ATP}}} \approx \frac{\nu_{\text{sat}}}{K_{\text{m}}} \cdot c_{\text{ATP}} \approx \text{const} \cdot c_{\text{ATP}},$$

which is the rate of the ATP consumption. c_{ATP} denotes here the ATP concentration, ν_{sat} is the inverse average time of a cycle, and K_{m} is the mechanochemical Michaelis–Menten constant. Thus the velocity of the kinesin is $v = \nu(c_{\text{ATP}})d$ (Fig. 3*b*).

The difference between the shapes of the force-velocity curves at saturating (Fig. 3 *a* and *c*) and at low (Fig. 3*b*) ATP concentration shows unambiguously the Fenn effect.

Changing the distribution of the load force F between the heads causes the change of the average time (t_{0L} and t_{L0}) needed for the two subprocesses, but their sum—i.e., the average duration t of the stepping cycle and the average displacement d—remains practically unchanged. Thus the force-velocity curves are essentially the same for any distribution of the load force.

We have also solved the Langevin equations (Eq. **1**) by *numerical* integration, and our values are in full agreement with the results obtained from the above analysis.

Discussion

Our model describes the stepping process of the kinesin molecule with elastically coupled heads. We do not use reaction rate constants, but only strain-induced conformational changes and the underlying asymmetric periodic potential. Therefore, we can give the full description of the dynamics of the motion.

From equation 7 of reference 11, it follows that the displacement variance of a two-step process (in which each cycle consists of two sequential subprocesses with comparable limiting rates) is $r = 1 - p_s/2$ times smaller than that of a single Poisson stepping process taking the same overall time. The stepping probability $p_s \leq 1$ denotes the probability that a cycle produces a forward step. In our model, at low load force the stepping probability is $p_s = p_{0L}^{+}p_{L0}^{+} \approx 0.8$; in addition, if the ATP concentration is saturated the two subprocesses are the only rate-limiting factors with the same rates. This leads to $r \approx 0.6$ as compared to $r \approx 0.52$ given with an error in the range of 0.1–0.2 in ref. 11. Thus, our model *explains the low displacement variance* at saturating ATP and at low load force. Furthermore, the model *fits the measured force-velocity curves* extremely well and is consistent with the recent experimental studies of the *pathway of the kinesin ATPase*. The parameters of the model are essentially determined by experiments or theoretical calculations; therefore, they can only be tuned in a rather restricted range. The shapes of the force-velocity curves are essentially insensitive to the parameters within this range, showing the robustness of the model.

If the relative position of the hinge to the backward head is fixed as, for example, in Fig. 2*b*, then only one power stroke occurs during one cycle. The main advantage of this version is that the hinge advances the whole 8-nm distance at once. (Note that in this case the first subprocess is not so important; thus it can be of a different type, for example, similar to the myosin step: detachment, free swinging, and rebinding to the next side.) In any other cases (like in Fig. 2*a*), the two subprocesses mean two power strokes, and the hinge advances the 8 nm in two parts. In spite of this, one may observe only 8-nm displacements, as the two power strokes occur in rapid succession.

From Eq. **2** it follows that the depth and the degree of asymmetry of the valleys in the periodic potential we assumed have the strongest effects on the results. On the other hand, some further details (such as, for example, a shallow secondary valley instead of the flat part) have less significant influence on the force–velocity curves. The temperature plays an essential role in the actual mechanism of the walk. The two major points where temperature comes into the picture are as follows: (*i*) the potential valley has to be considerably deeper than $3kT$ to ensure proper binding, (*ii*) on the other hand, from a deep valley the heads may escape only if the spring and the temperature act simultaneously since the energy of the spring cannot be larger than that of the ATP hydrolysis.

To decide which theoretical model describes the kinesin stepping process in the best way, further experimental studies are needed. One possibility is to see how the force–velocity curves continue both at higher forces than the stall force and at negative forces. Another possibility is to measure the displacement variance at higher loads and at lower ATP concentrations. This could distinguish among the different cases of our model as well, because for different distributions of the load force F the average duration of the subprocesses are also different resulting in different variances.

We are aware that C. Doering, M. Magnasco and G. Oster (personal communication) have considered a similar approach to the problem of the kinesin walk.

We are grateful to J. Prost and A. Ajdari for useful discussions and for their kind hospitality during the visit of I.D. at Ecole Supérieure de Physique et de Chimie Industrielles in Paris. The present research was supported by the Hungarian Research Foundation (Grants T4439 and F17246), and Contract ERB-CHRX-CT92–0063.

1. Darnell, J., Lodish, H. & Baltimore, D. (1990) *Molecular Cell Biology* (Sci. Am. Books, New York).
2. Song, Y.-H. & Mandelkow, E. (1993) *Proc. Natl. Acad. Sci. USA* **90,** 1671–1675.
3. Hoenger, A., Sablin, E. P., Vale, R. D., Fletterick, R. J. & Milligan, R. A. (1995) *Nature (London)* **376,** 271–274.
4. Kikkawa, M., Ishikawa, T., Wakabayashi, T. & Hirokawa, N. (1995) *Nature (London)* **376,** 274–277.
5. Hirose, K., Lockhart, A., Cross, R. A. & Amos, L. A. (1995) *Nature (London)* **376,** 277–279.
6. Vale, R. D., Reese T. S. & Sheetz M. P. (1985) *Cell* **42,** 39–50.
7. Ray, S., Meyhoefer, E., Milligan, R. A. & Howard, J. (1993) *J. Cell Biol.* **121,** 1083–1093.
8. Hunt, A. J., Gittes, F. & Howard, J. (1994) *Biophys. J.* **67,** 766–781.
9. Svoboda, K. & Block, S. M. (1994) *Cell* **77,** 773–784.
10. Svoboda, K., Schmidt, C. F., Schnapp, B. J. & Block, S. M. (1993) *Nature (London)* **365,** 721–727.

11. Svoboda, K., Mitra, P. P. & Block, S. M. (1994) *Proc. Natl. Acad. Sci. USA* **91,** 11782–11786.
12. Magnasco, M. O. (1993) *Phys. Rev. Lett.* **71,** 1477–1480.
13. Ajdari, A. & Prost, J. (1992) *C.R. Acad. Sci. Paris* **315,** 1635–1639.
14. Prost, J., Chauwin, J.-F., Peliti, L. & Ajdari, A. (1994) *Phys. Rev. Lett.* **72,** 2652–2655.
15. Astumian, R. D. & Bier, M. (1994) *Phys. Rev. Lett.* **72,** 1766–1769.
16. Doering, C. R., Horsthemke, W. & Riordan, J. (1994) *Phys. Rev. Lett.* **72,** 2984–2987.
17. Millonas, M. M. & Dykman, D. I. (1994) *Phys. Lett. A* **185,** 65–69.
18. Millonas, M. M. (1995) *Phys. Rev. Lett.* **74,** 10–13.
19. Bartussek, R., Hänggi, P. & Kissner, J. G. (1994) *Europhys. Lett.* **28,** 459–464.
20. Ajdari, A. (1994) *J. Phys.* **4,** 1577–1582.
21. Block, S. M. & Svoboda, K. (1995) *Biophys. J.* **68,** 230–241.
22. Peskin, C. S. & Oster, G. (1995) *Biophys. J.* **68,** 202–211.
23. Rayment, I., Holden, H. M., Whittaker, M., Yohn, C. B., Lorenz, M., Holmes, K. C. & Milligan, R. A. (1993) *Science* **261,** 58–65.
24. Ostap, E. M. & Thomas, D. D. (1995) *Biophys. J.* **68,** 335.
25. Gilbert, S. P., Webb, M. R., Brune, M. & Johnson, K. A. (1995) *Nature (London)* **373,** 671–676.
26. Fenn, W. O. (1924) *J. Physiol. (London)* **184,** 373–395.